Talanta 200 (2019) 300–306

Contents lists available at ScienceDirect

Talanta

journal homepage: www.elsevier.com/locate/talanta

Green and low-cost synthesis of nitrogen-doped graphene-like mesoporous nanosheets from the biomass waste of okara for the amperometric detection of vitamin C in real samples

Tianze Sha[a], Jingju Liu[a], Mimi Sun[a], Lei Li[d], Jing Bai[a,*], Zongqian Hu[c,*], Ming Zhou[a,b]

[a] Key Laboratory of Nanobiosensing and Nanobioanalysis at Universities of Jilin Province, Key Laboratory of Polyoxometalate Science of Ministry of Education, National & Local United Engineering Laboratory for Power Batteries, Department of Chemistry, Northeast Normal University, Changchun, Jilin Province 130024, PR China
[b] School of Chemistry and Environmental Engineering, Jilin Provincial Science and Technology Innovation Center of Optical Materials and Chemistry, Changchun University of Science and Technology, Changchun, Jilin Province 130022, PR China
[c] Beijing Institute of Radiation Medicine, Beijing 100850, PR China
[d] The College of Electrical and Electronic Engineering, Advanced Institute of Materials Science, Changchun University of Technology, Changchun, Jilin Province 130012, PR China

ARTICLE INFO

Keywords:
Biomass waste
Electrochemical biosensor
Nanosheets
Vitamin C

ABSTRACT

In this work, the low-cost nitrogen-doped graphene-like mesoporous nanosheets (N-GMNs) was synthesized from the biomass waste of okara for the first time for the construction of a nonenzymatic amperometric vitamin C biosensor. The N-GMNs modified glassy carbon electrode (N-GMNs/GCE) shows much lower overpotential for the electrooxidation of vitamin C comparing to the traditional GCE as well as the GCE modified by carbon nanotubes (CNTs/GCE), indicating the promising of N-GMNs/GCE for the sensitive and selective nonenzymatic amperometric vitamin C biosensing. As a nonenzymatic amperometric biosensor for vitamin C, the N-GMNs/GCE shows a higher sensitivity (144.65 $\mu A\,mM^{-1}\,cm^{-2}$), a wider linear range (10–5640 $\mu mol\,L^{-1}$) and a lower detection limit (0.51 $\mu mol\,L^{-1}$) than GCE, CNTs/GCE or some of recently reported nanomaterials-based electrochemical vitamin C biosensors. Especially, the vitamin C concentration in real samples of commercial beverage, vitamin C injection and commercial juice can be determined by the proposed N-GMNs/GCE with satisfied results. Therefore, the utilization of okara as the raw material for the synthesis of nanostructured carbon of N-GMNs is a green method to fabricate an advanced and low-cost electrode material for developing the nonenzymatic electrochemical biosensor for vitamin C detection.

1. Introduction

Vitamin C is also called as ascorbic acid which plays a significant role in the biological metabolism. For example, vitamin C often participates in human physiological processes and it has been commonly employed for the treatment of psychological illness, cancer, infertility and Acquired Immune Deficiency Syndrome (AIDS), etc. [1]. In addition, vitamin C is also used as the essential antioxidant in different commercial products, such as beverages, animal feed, cosmetics and food pharmaceutical formulations [2,3]. Therefore, vitamin C detection is important for both human health [4] and medical industries [5]. Nowadays, different techniques have been used for molecules/biomolecules detection (for example, mass spectrometry [6], spectrophotometry [7,8], solid phase iodine [9], chromatography [10], chemiluminescence [11–14] and electrochemical method [15–20]). Among these methods, the electrochemical one with many unique features of simple operation and high selectivity is very attractive [21]. However, the overvoltage for vitamin C electrooxidation at carbon based electrode (e.g., glassy carbon and graphite) is usually high, which often results in low sensitivity, poor reproducibility and electrode fouling [22]. To overcome these limitations, noble metals are usually applied as the electrocatalysts for the construction of electrochemical vitamin C biosensors with improved analytical performance [23]. Nevertheless, the limited reservation over the world and the high cost of noble metal may impede the mass application. In consequence, developing cost-efficient and environmentally-friendly electrocatalysts with high performance for electrochemical sensing is necessary.

According to the U.S. National Nanotechnology Initiative definition, nanomaterial is a kind of materials which has at least one dimension from one to a hundred nanometers range [24–28]. Due to their special

* Corresponding authors.
E-mail addresses: baij243@nenu.edu.cn (J. Bai), huzongqian@hotmail.com (Z. Hu), zhoum739@nenu.edu.cn (M. Zhou).

https://doi.org/10.1016/j.talanta.2019.03.071
Received 11 December 2018; Received in revised form 13 March 2019; Accepted 16 March 2019
Available online 16 March 2019
0039-9140/

nanostructure characteristics, the nanomaterials have been widely used in various applications including electrochemical sensing [29], biosensing [30], energy [31], environmental issues [32–34] and etc. [35–37]. Since the discovery of zero dimensional (0-D) fullerenes [38] in last century, carbon nanomaterials with different dimensions have been introduced in electrochemistry [39]. Although this kind of nanomaterials exhibited the very attractive electroanalytical capabilities, the high cost of the pure reagents, a complicated fabrication process and a number of synthetic steps for carbon nanomaterials synthesis probably limit their practical and mass applications [40].

As the renewable organic materials, biomass was derived from plants or animals [41]. Recently, the carbon based materials from biomass especially organic wastes (sunflower seed shell [42], dead ginkgo leaves [43], wheat straw [44] and etc.) have caused great attention because of their environmental-friendly and reasonable cost characters. This kind of materials exhibits environmentally-friendly and cost-efficient features. Additionally, they have many advantages such as excellent chemical stability, low toxicity and high surface area, which could benefit for exploring their applications in various fields, such as energy storage [45], catalysis [46], adsorption [47] and environmental science [48]. The relative studies have showed ta large extent about developing biomass-derived carbon-based materials in electrochemistry.

Okara is a kind of byproducts/wastes from the manufacture process of soybean oil, soy milk or tofu. Every year, China, U.S., and Brazil plant billions bushels of soybeans, which leads to a large number of okara wastes [49] and results in rising environmental and ecological problems. In this study, the nitrogen-doped graphene-like mesoporous nanosheets (N-GMNs) was derived from the biomass waste of okara which was synthesized for electrochemical vitamin C biosensing for the first time. The okara was applied as the both carbon and nitrogen sources of N-GMNs. The N-GMNs modified GCE (N-GMNs/GCE) exhibits a lower overpotential in comparison with glassy carbon electrode (GCE) and GCE modified by carbon nanotubes (CNTs/GCE). For vitamin C determination, because of the improved electrochemistry activity, the N-GMNs/GCE shows lower detection limit, higher sensitivity and wider linear range than GCE and CNTs/GCE. Additionally, the obtained electrochemical sensor can be able to sensitively and selectively detect vitamin C in vitamin C injection, commercial beverage and commercial juice with satisfying results.

2. Experimental section

2.1. Reagents and materials

The soybeans (*Glycine max*) were bought in a local market. Carbon nanotubes (CNTs, 5 wt% in N,N-dimethylformamide (DMF)) solution was purchased from Beijing Dk Nano technology Co., Ltd. Vitamin C was purchased from Sinopharm Chemical Reagent Co. Ltd. The vitamin C medical injection was obtained from Bingchenglongke Veterinary Drugs Ltd. (P.R. China). The commercial beverage (Nongfu Spring Co., Ltd, P.R. China) and the commercial juice (Bestshin Beverages Co., Ltd, P.R. China) were both obtained in the Northeast Normal University campus market, which is located in Changchun, China. All chemical reagents were used as received without further purification.

2.2. Apparatus and measurements

The working electrodes were glassy carbon electrode (GCE, 3 mm diameter), the CNTs modified GCE (CNTs/GCE) and the N-GMNs modified GCE (N-GMNs/GCE). A Pt wire and Ag/AgCl (in saturated KCl solution) electrode were applied as counter and reference electrodes, respectively. The other equipment applied in this work were the same with those reported by our group [50].

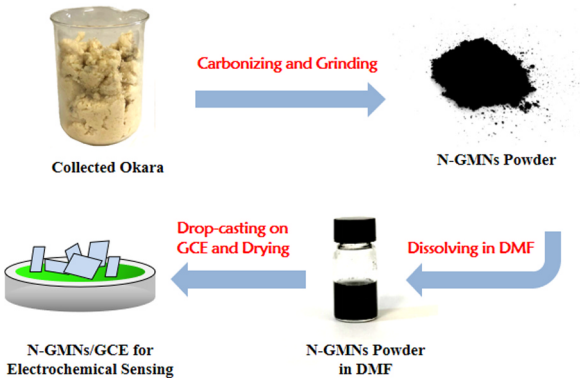

Scheme 1. Synthesis of N-GMNs for electroanalysis.

2.3. Synthesis of nitrogen-doped graphene-like mesoporous nanosheets (N-GMNs) from the biomass waste of okara

Firstly, the fresh okara was dried by keeping the samples in an oven at 60 °C overnight. After treating the dried okara in a tubular furnace at 800 °C under nitrogen atmosphere for 2 h, then the N-GMNs was obtained.

2.4. Electrode modification

GCE was firstly cleaned by aluminum oxide powder before each modification, which was similar with that reported by our group [50]. After grounding the N-GMNs, the powder was dispersed in DMF to obtain the N-GMNs suspension (Scheme 1). N-GMNs/GCE was obtained by casting the N-GMNs suspension onto GCE and dried under an infrared lamp. In order to obtain high electrochemical performance of N-GMNs/GCE, the ratio of the weight of N-GMNs to the volume of DMF and the volume of N-GMNs suspension were both explored by electrochemical impedance spectroscopy. 5 μL of 10 mg mL^{-1} suspension showed lowest electron transfer resistance in the solution containing 5 mmol L^{-1} $Fe(CN)_6^{3-/4-}$ and 0.1 mol L^{-1} KCl (data not shown). For control experiments, the CNTs/GCE was prepared by the similar method/parameters compared to N-GMNs/GCE. Additionally, the concentration of CNTs/DMF was also chosen as 10 mg mL^{-1}, then 5 μL of CNTs/DMF dispersion was dropped on the clean surface of GCE and dried under an infrared lamp.

3. Results and discussion

3.1. Characterization of biomass waste of nitrogen-doped graphene-like mesoporous nanosheets (N-GMNs)

The microstructure of N-GMNs was first characterized by the transmission electron microscope (TEM). As shown in Fig. 1A, the N-GMNs possesses the typical morphology of graphene-like sheets with a wrinkled structure. Fig. 1B exhibits the nitrogen (N_2) adsorption-desorption isotherms of the N-GMNs. The N-GMNs shows the type IV curves with an obvious H_4 hysteresis loop at a P/P_0 of 0.45–1.0, indicating the presence of mesopores in N-GMNs [51,52]. In addition, the N-GMNs exhibits a high BET surface area (133 m^2 g^{-1}) with mesopores (centered at 2.56 nm) (Fig. 1C). The porous, wrinkled and graphene-like microstructure of N-GMNs could be very favorable to electroanalysis [53–56].

The microstructure of N-GMNs was further investigated by the X-ray diffraction (XRD). As shown, the N-GMNs represents two broad diffraction peaks centered at ~24° and ~43°, respectively (Fig. 2A), corresponding to the (002) and (101) planes [57]. Fig. 2B indicates the

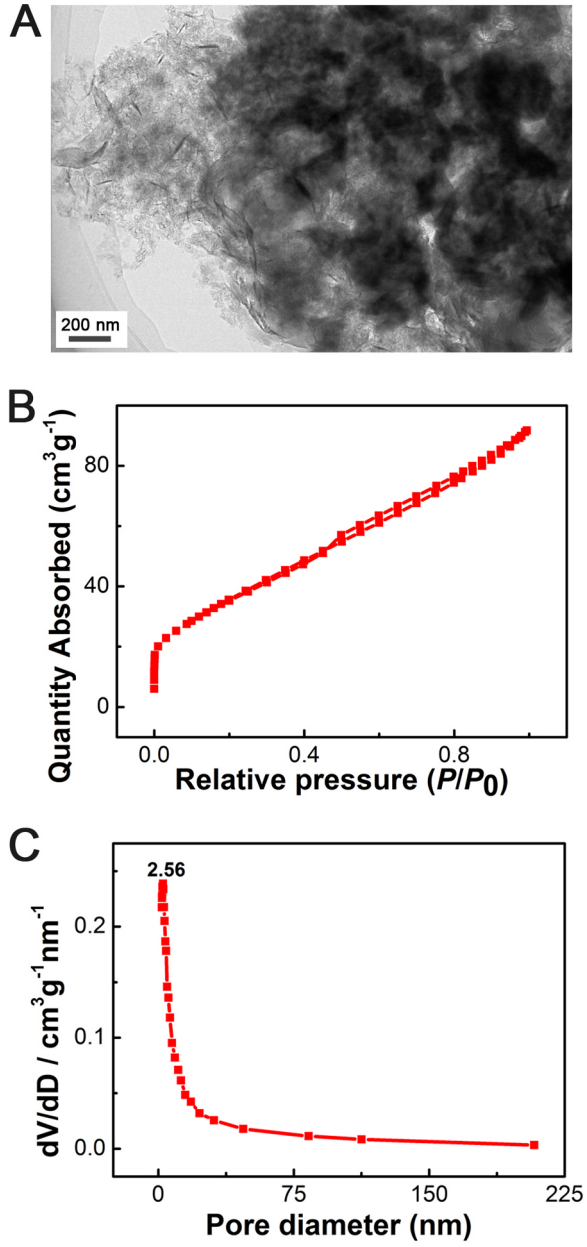

Fig. 1. (A) TEM image of N-GMNs. (B) N_2 adsorption-desorption isotherms of N-GMNs. (C) The pore size distribution of N-GMNs.

Raman spectrum of N-GMNs. As shown, the D band at 1352 cm^{-1} represents the crystal defects in materials, involving in the sp^2 atom in the carbon ring [58]; the G band at 1578 cm^{-1} is related to the graphite layer, which associates to the vibration of the E_{2g} symmetry. In general, the relative intensity ratio of the D band and the G band (I_D/I_G) is proportional to the number of defective sites of carbon materials. The I_D/I_G value of N-GMNs is 1.092 (Fig. 2B), which is higher than that of CNTs (0.999 [59]), vapor grown carbon fibers (0.860 [60]) or mesoporous carbons (0.700 [61]). A high I_D/I_G value suggests that the N-GMNs possesses a high density of defective sites, which might be favorable for the electrocatalysis.

The surface chemistry of N-GMNs was also investigated by the X-ray photoelectron spectroscopy (XPS). As shown in Fig. 2C, the N-GMNs is consisted of the C, O and N elements, and the relative atom percentage of C, O and N in N-GMNs is 88.40%, 9.43% and 2.17%, respectively. Fourier transform infrared (FTIR) spectroscopy in Fig. 2D suggests that the bands at 1380 cm^{-1} and 3442 cm^{-1} corresponds to C–N stretching vibration [62] and the band at 1638 cm^{-1} is signed to the asymmetric C = O stretching bands [63] in N-GMNs. In addition, the peaks around 2953 cm^{-1} and 2854 cm^{-1} relate to the asymmetric and symmetric stretching vibrations of -CH_2 resulting from the edges of N-GMNs which may arise because of the presence of amorphous carbon [64].

3.2. Electrochemical reactivity

As shown in Fig. 3A, the potential difference ($^{\triangle}E_p$) between the anodic and cathodic peaks at N-GMNs modified glassy carbon electrode (N-GMNs/GCE, 72 mV) in KCl solution containing $K_3Fe(CN)_6^{-3/-4}$ is lower than that at GCE modified by carbon nanotubes (CNTs/GCE, 85 mV) or glassy carbon electrode (GCE, 90 mV), which indicates the faster electron transfer rate at N-GMNs/GCE comparing to GCE or CNTs/GCE [65]. According to Nicholson's equation [65],

$$k^0 = \frac{\Psi\left[D_o\pi\left(\frac{nFv}{RT}\right)\right]^{1/2}}{\left(\frac{D_o}{D_r}\right)^{\alpha/2}} \quad (1)$$

where k^0 is the heterogeneous electron transfer rate, Ψ is the dimensionless kinetic parameter determined from ΔEp, D_o/D_r are the diffusion coefficients of the oxidized/reduced form of the electroactive species, α is the transfer coefficient, n is the number of electrons transferred in this electrochemical reaction ($n = 1$), F is the Faraday constant ($F = 96{,}489$ C mol^{-1}), v is the scan rate in V s^{-1} ($v = 10$ mV s^{-1}), R is the universal gas constant ($R = 8.314$ J K^{-1} mol^{-1}) and T is the absolute Temperature ($T = 273$ k). Assuming the D_o and D_r to be approximately equal (For 5 mmol L^{-1} $K_3Fe(CN)_6$ contained 0.1 mol L^{-1} KCl electrolyte, $D_o = 6.6 \times 10^{-6}$ cm^2 s^{-1}) and symmetrical redox kinetics ($\alpha \approx 0.5$) of the redox mediator, the above equation simplifies to:

$$k^0 = \Psi\sqrt{D_o\pi\left(\frac{nFv}{RT}\right)} \quad (2)$$

For a one electron process, Ψ depends on ΔEp and can be determined from the following equation:

$$\Psi = \frac{(-0.6288 + 0.0021X)}{(1 - 0.017X)} \quad (3)$$

where X is equal to the peak potential separation (ΔEp) of the system multiplied by the number of electrons involved in the electrochemical reaction.

By combining Eqs. (1)–(3) above, k^0 at N-GMNs/GCE, CNTs/GCE and GCE were calculated to be 0.00752 cm s^{-1}, 0.00279 cm s^{-1} and 0.00214 cm s^{-1}, respectively. That means the presence of N-GMNs on GCE plays a key role in providing the electron-transfer bridges between electrode and electrochemical probe. In addition, based on Randles-Sevcik equation below [66]:

$$I_{pa} = 2.69 \times 10^5 n^{3/2} C_0 D^{1/2} A\, v^{1/2} \quad (4)$$

where, I_{pa} refers to the anodic peak current (A), n is the electron transfer number, A represents the apparent surface area of the electrode (cm^2), D is the diffusion coefficient, C_o (mol L^{-1}) is the concentration of $K_3Fe(CN)_6$ and v is the scan rate (V s^{-1}). For 5 mmol L^{-1} $K_3Fe(CN)_6$ containing 0.1 mol L^{-1} KCl electrolyte: $n = 1$ and $D = 6.6 \times 10^{-6}$ cm^2 s^{-1}, $v = 10$ mV s^{-1}. According to Randles-Sevcik equation, the apparent surface area of N-GMNs/GCE is calculated to be 0.097 cm^2, which is higher than that of CNTs/GCE (0.075 cm^2) or GCE (0.070 cm^2).

Vitamin C is usually used as the antioxidants in animal feed, beverages, food, cosmetic applications and pharmaceutical formulations [50]. In addition, vitamin C has been also commonly used for the prevention of mental illness, cancer, infertility, Acquired Immune

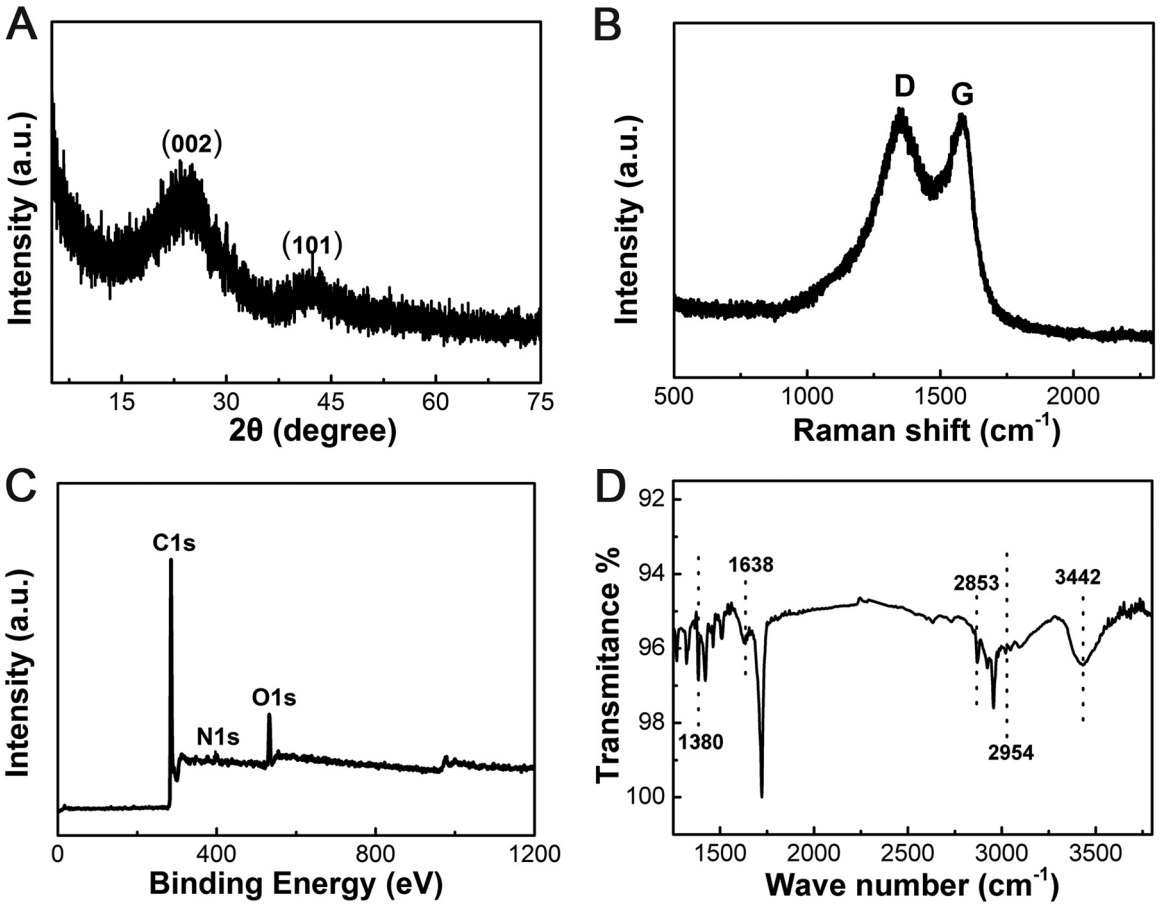

Fig. 2. (A) XRD pattern of N-GMNs. (B) Raman spectrum of N-GMNs. (C) XPS spectrum of N-GMNs. (D) FT-IR spectrum of N-GMNs.

Deficiency Syndrome (AIDS), and etc. [1]. So the accurate detection of vitamin C in real samples is significant. Firstly, we investigated the electrocatalysis of vitamin C at different electrodes. Fig. 3B shows the CV curves in the presence and absence of vitamin C at N-GMNs/GCE, CNTs/GCE and GCE. As shown, a well-defined peak for vitamin C electrooxidation can be observed at each electrode when vitamin C was present (solid lines in Fig. 3B) but no obvious peaks can be found for the blank measurement (dotted lines in Fig. 3B), which means that the obtained peak at each electrode corresponds to the presence of vitamin C. The anodic potentials at N-GMNs/GCE, CNTs/GCE and GCE are +0.001 V, +0.266 V and +0.343 V, respectively. And the peak current at N-GMNs/GCE is ~1.6-fold higher than that of CNTs/GCE or ~1.8-fold higher than that of GCE. It should be noteworthy that compared to GCE and CNTs/GCE, the N-GMNs/GCE not only shows the highest peak current but also displays the lowest peak potential for vitamin C electrooxidation. Thus, the N-GMNs/GCE possesses the highest electrocatalytic activity towards the vitamin C electrooxidation among three electrodes, which reveals the high sensitivity and selectivity for the amperometric vitamin C determination at N-GMNs/GCE.

3.3. Determination of vitamin C

The electroanalytical performances at N-GMNs/GCE, CNTs/GCE and GCE to vitamin C determination were investigated by the amperometric technique (Fig. 4A). The N-GMNs/GCE exhibited lower detection limit of 0.51 μmol L^{-1} (S/N = 3), wider linear relationship from 10 to 5640 μmol L^{-1} (with the slope of 0.0102 μA μmol L^{-1}) and higher sensitivity of 144.65 μA mmol L^{-1} cm^{-2} comparing to CNTs/GCE or GCE. The analytical performance of N-GMNs/GCE for vitamin C detection was also compared to some recently reported nanomaterials-based electrochemical biosensors, Table 1. The analytical performance of N-GMNs/GCE is superior.

As is known that some biomolecules may show serious interference for the electrochemical detection of vitamin C [77]. So the interference effect of some biomolecules to vitamin C detection at N-GMNs/GCE was also investigated. Fig. 4B represents the current responses at N-GMNs/GCE with sequentially added 0.1 mmol L^{-1} vitamin C and other biomolecules at +0.001 V in N_2-saturated PBS. After the injection of 0.1 mmol L^{-1} vitamin C, the oxidation current apparently increased, but the presence of other biomolecules did not lead to obvious current change, demonstrating no interference for vitamin C detection at N-GMNs/GCE. The anti-fouling capability of the biosensor is another essential factor for the electrochemical sensing [78]. As shown in Fig. 4C, after 5 h, there was a remarkable 34% current declining of CNTs/GCE. On the contrary, N-GMNs/GCE still remained 80% of the initial value. The outstanding analytical performance of N-GMNs/GCE for vitamin C detection mentioned above suggests its highly promising potential for the amperometric detection of vitamin C in real samples.

3.4. Real samples detection

To evaluate the feasibility of the present biosensor for real application, the vitamin C detection in vitamin C injection, commercial beverage or commercial juice was performed. The utilization of the standard addition method was used for direct analysis of the real samples without any pretreatments, and the analysis results were listed

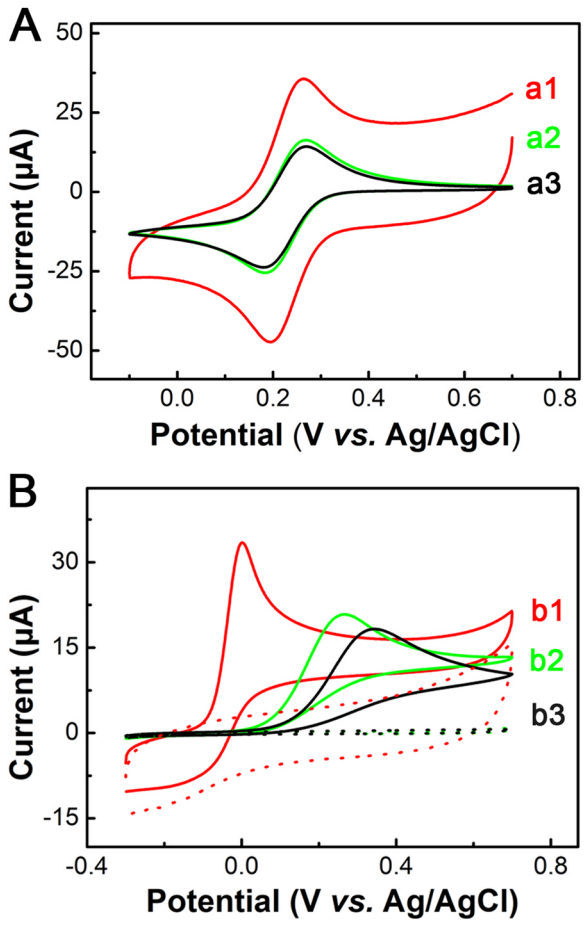

Fig. 3. (A) CV curves of N-GMNs/GCE (a1), CNTs/GCE (a2) and GCE (a3) in a solution of 5 mmol L^{-1} $K_3Fe(CN)_6^{-3/-4}$ and 0.1 mol L^{-1} KCl. (B) CV curves of 2.5 mmol L^{-1} vitamin C (solid lines) for N-GMNs/GCE (b1), CNTs/GCE (b2) and GCE (b3) in N_2-saturated 0.1 mol L^{-1} pH 7.0 PBS. Dotted lines represent the blank measurements. Scan rate: 10 mV s^{-1}.

in Table 2. As shown, the recoveries for the three samples are between 96% and 101%, indicating the sensitive and effective detection for vitamin C [50]. In particular, the vitamin C concentration in vitamin C medical injection, beverage or juice samples detected by N-GMNs/GCE was consistent with the information offered by the products company, suggesting the high accuracy for vitamin C detection at such amperometric biosensor. All of those results indicate the high possibility of the N-GMNs/GCE for the accurate vitamin C detection in different fields from foodstuffs safety to human health diagnostics. However, the buffer solution is still required, which means that such sensor may not determine AA in vivo.

4. Conclusion

To conclude, a biomass waste of okara derived nanomaterial of N-GMNs as a novel electrode material with high density of edge-plane-like defective sites, large surface area and uniform mesopores was synthesized for the electrooxidation and amperometric detection of vitamin C. The N-GMNs/GCE exhibits superior analytical performance with wider linear range (10–5640 μmol L^{-1}), lower detection limit (0.51 μmol L^{-1}) and better sensitivity (144.65 μA mmol L^{-1} cm^{-2}) than the GCE, CNTs/GCE or some recently reported nanomaterials-based electrochemical vitamin C biosensors. Most importantly, the proposed biosensor is able to test vitamin C in some real samples of commercial beverage, vitamin C injection and commercial juice with satisfactory results, demonstrating the high possibility of N-GMNs as a kind of novel and reasonable cost carbon material to detect vitamin C in food analysis or pharmaceutical industry. Therefore, the utilization of okara as the raw material for the synthesis of nanostructured carbon of N-GMNs is a green method to fabricate an advanced and low-cost electrode material for developing the nonenzymatic electrochemical biosensor for vitamin C detection.

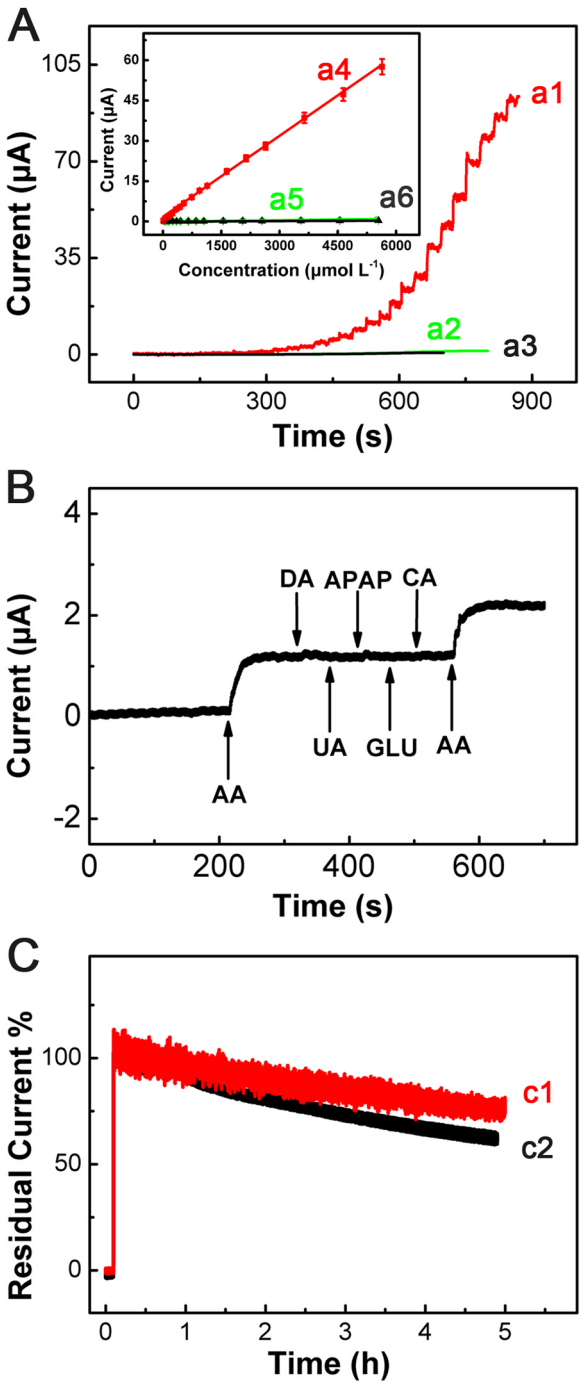

Fig. 4. (A) Typical amperometric responses of N-GMNs/GCE (a1), CNTs/GCE (a2) and GCE (a3) to successive addition of vitamin C at +0.001 V. Inset: the calibration curves for N-GMNs/GCE (a4), CNTs/GCE (a5) and GCE (a6). (B) Current-time curves for N-GMNs/GCE to successive additions of 0.1 mmol L^{-1} vitamin C, 0.15 mmol L^{-1} DA, 0.1 mmol L^{-1} UA, 0.1 mmol L^{-1} APAP, 1 mmol L^{-1} glucose and 0.1 mmol L^{-1} CA at +0.001 V. (C) Current-time curves of 0.5 mmol L^{-1} vitamin C for N-GMNs/GCE (c1) and CNTs/GCE (c2) at +0.001 V. All experiments were studied in N_2-saturated 0.1 mol L^{-1} pH 7.0 PBS with magnetically stirred.

Table 1
Analytical performances of different nanomaterials-based electrochemical vitamin C biosensors.

Species	Electrode	Linear range (μmol L^{-1})	Sensitivity (μA mmol L^{-1})	Detection limit (S/N = 3) (μmol L^{-1})	References
Vitamin C	N-GMNs/GCE	10–5640	10.23	0.51	This work
	CNTs/GCE	50–5550	0.117	7.59	This work
	GCE	50–5550	0.056	51.80	This work
	CoHCF/GCE	55.2–32300	/	33.3	[67]
	AuNPs/HDT/Au	1.0–110	/	1.0	[68]
	Polypyrrole/ Naphthol green B/GCE	240–25000	7	/	[69]
	$Fe(CN)_6^{3-}$/PAH/PSS–$CaCO_3$/CS/GCE	1.0–2143	4	0.7	[70]
	MWCNT/CCE	15–800	41.3	7.71	[71]
	Poly (allylamine) ferrocene/Au electrode	50–1000	/	27.0	[72]
	Cu-NPs/PANI/GCE	5.0–3500	/	2.0	[73]
	Organoclay film/GCE	70–1100	/	10	[74]
	[DCPI] 3-La/SPCE	10–1000	/	10	[75]
	CoPc–MWCNTs/ GCE	10–2600	/	1.0	[4]
	Surface-immobilized PFS chains modified electrode	5–40	/	5.0	[76]

CoHCF, cobalt hexacyanoferrate; HDT, 1,6-Hexanedithiol; AuNPs, gold nanoparticles; PAH, poly hydrochloride; PSS–$CaCO_3$, prepared poly (sodium 4-styrenesulfonate)-doped porous calcium carbonate; CS, chitosan; MWCNT/CCE, multiwalled carbon nanotube modified carbon-ceramic electrode; Cu-NPs, copper nanoparticles; PANI, polyaniline; [DCPI] 3La, 2,6-dichlorophenolindophenol lanthanum salt; SPCE, screen printed carbon electrode; CoPc, Cobalt (II) phthalocyanine; PFS, poly (ferrocenylsilane).

Table 2
Detection of vitamin C in real samples.

Sample	Provided by companies (μmol L^{-1})	Detected (μmol L^{-1})	Added (μmol L^{-1})	After added (μmol L^{-1})	Mean recovery (%)
Vitamin C injection	68.13	68.81	0	68.81	100.99
			70	136.58	98.88
			140	207.23	99.57
			210	270.59	97.29
Beverage	127.50	125.81	0	125.81	98.67
			70	193.61	98.03
			140	262.60	98.17
			210	324.74	96.22
Juice	89.40	87.49	0	87.49	97.86
			70	154.92	97.19
			140	221.35	96.49
			210	290.99	97.19

Acknowledgements

The authors gratefully acknowledge the supports from the National Natural Science Foundation of China (21605015), the Development Project of Science and Technology of Jilin Province (20170101176JC), the Fundamental Research Funds for the Central Universities (2412017BJ003), the project of Jilin Province Science and Technology Department Outstanding Young Talents Foundation (20170520160JH), the Recruitment Program of Global Youth Experts, the Jilin Provincial Department of Education, the start-up funds from Northeast Normal University, and the Analysis and Testing Center of Northeast Normal University.

References

[1] M.B. Davies, J. Austin, D.A. Partridge, Vitamin C: Its Chemistry and Biochemistry, Royal Society of Chemistry, 1991.
[2] A.M. Pisoschi, A. Pop, A.I. Serban, C. Fafaneata, Electrochemical methods for ascorbic acid determination, Electrochim. Acta 121 (2014) 443–460.
[3] L. Özcan, M. Sahin, Y. Sahin, Electrochemical preparation of a molecularly imprinted polypyrrole-modified pencil graphite electrode for determination of ascorbic acid, Sensors 8 (9) (2008) 5792–5805.
[4] X. Zuo, H. Zhang, N. Li, An electrochemical biosensor for determination of ascorbic acid by cobalt (II) phthalocyanine–multi-walled carbon nanotubes modified glassy carbon electrode, Sens. Actuators B: Chem. 161 (1) (2012) 1074–1079.
[5] S. Qiu, S. Gao, Q. Liu, Z. Lin, B. Qiu, G. Chen, Electrochemical impedance spectroscopy sensor for ascorbic acid based on copper (I) catalyzed click chemistry, Biosens. Bioelectron. 26 (11) (2011) 4326–4330.
[6] J.M. Conley, S.J. Symes, S.A. Kindelberger, S.M. Richards, Rapid liquid chromatography–tandem mass spectrometry method for the determination of a broad mixture of pharmaceuticals in surface water, J. Chromatogr. A 1185 (2) (2008) 206–215.
[7] K. Güçlü, K. Sözgen, E. Tütem, M. Özyürek, R. Apak, Spectrophotometric determination of ascorbic acid using copper (II)–neocuproine reagent in beverages and pharmaceuticals, Talanta 65 (5) (2005) 1226–1232.
[8] M. Tian, X. Guo, R. Wang, Preparation of test paper for rapid determination of ammoniacal nitrogen in water by electrostatic spinning method, J. Mol. Sci. 34 (01) (2018) 49–53.
[9] M. Noroozifar, M. Khorasani-Motlagh, Solid-phase iodine as an oxidant in flow injection analysis: determination of ascorbic acid in pharmaceuticals and foods by background correction, Talanta 61 (2) (2003) 173–179.
[10] A.G. Frenich, M.H. Torres, A.B. Vega, J.M. Vidal, P.P. Bolanos, Determination of ascorbic acid and carotenoids in food commodities by liquid chromatography with mass spectrometry detection, J. Agric. Food Chem. 53 (19) (2005) 7371–7376.
[11] A.F. Dänet, M. Badea, H.Y. Aboul-Enein, Flow injection system with chemiluminometric detection for enzymatic determination of ascorbic, Luminescence 15 (2000) 305–309.
[12] J. Li, J. Ma, Y. Zhang, Z. Zhang, G. He, A fluorometric method for determination of the activity of T4 polynucleotide kinase by using a DNA-templated silver nanocluster probe, Microchim. Acta 186 (1) (2019) 48.
[13] M. Moßhammer, K.E. Brodersen, M. Kühl, K. Koren, Nanoparticle- and microparticle-based luminescence imaging of chemical species and temperature in aquatic systems: a review, Microchim. Acta 186 (2) (2019) 126.
[14] D. Zhu, Y. Hu, X.-J. Zhang, X.-T. Yang, Y.-Y. Tang, Colorimetric and fluorometric dual-channel detection of α-fetoprotein based on the use of ZnS-CdTe hierarchical porous nanospheres, Microchim. Acta 186 (2) (2019) 124.
[15] D. Zhao, G. Yu, K. Tian, C. Xu, A highly sensitive and stable electrochemical sensor for simultaneous detection towards ascorbic acid, dopamine, and uric acid based on the hierarchical nanoporous PtTi alloy, Biosens. Bioelectron. 82 (2016) 119–126.
[16] K. Wu, J. Sun, Y. Tian, Z. Guo, Y. Hu, Y. Qi, L. Tian, Determination of p-nitrophenol on electrochemical luminescence sensor based on GO-CdTe, J. Mol. Sci. 35 (01) (2019) 49–55.
[17] Y. Zhu, G. Yang, B. Han, B. Qi, Electroanalytical determination of ofloxacin using gold nanoparticles loaded carbon nanofibers, J. Mol. Sci. 34 (04) (2018) 338–342.
[18] Y. Du, H. Li, Y. Xie, Y. Feng, X. Du, B. Qi, Development of an unique Ru(bpy)32+/OMC-Nafion/GCE sensor for electrochemical detection of ephedrine hydrochloride, J. Mol. Sci. 34 (01) (2018) 59–63.
[19] Y. Wang, Y. Xia, Optical, electrochemical and catalytic methods for in-vitro diagnosis using carbonaceous nanoparticles: a review, Microchim. Acta 186 (1) (2019) 50.
[20] H. Huang, T. Li, Y. Sun, L. Yu, C. Wang, R. Shen, W. Ye, D. Wang, Y. Li, Amperometric sensing of hydrazine in environmental and biological samples by using CeO2-encapsulated gold nanoparticles on reduced graphene oxide, Microchim. Acta 186 (1) (2019) 46.
[21] X. Zhang, Y. Cao, S. Yu, F. Yang, P. Xi, An electrochemical biosensor for ascorbic acid based on carbon-supported PdNi nanoparticles, Biosens. Bioelectron. 44 (2013) 183–190.
[22] L. Tian, L. Chen, L. Liu, N. Lu, W. Song, H. Xu, Electrochemical determination of ascorbic acid in fruits on a vanadium oxide polypropylene carbonate modified electrode, Sens. Actuators B: Chem. 113 (1) (2006) 150–155.
[23] G.-h. Wu, Y.-f. Wu, X.-w. Liu, M.-c. Rong, X.-m. Chen, X. Chen, An electrochemical ascorbic acid sensor based on palladium nanoparticles supported on graphene oxide, Anal. Chim. Acta 745 (2012) 33–37.
[24] W. Zhang, S. Zhu, R. Luque, S. Han, L. Hu, G. Xu, Recent development of carbon electrode materials and their bioanalytical and environmental applications, Chem. Soc. Rev. 45 (3) (2016) 715–752.
[25] Z. Qiang, B. Ma, R. Wang, L. Li, The influence of magnetic field on microcosmic diffusion characteristics of electrolyte in electrochemical reaction, J. Mol. Sci. 35 (01) (2019) 70–76.

[26] S. Lv, T. Kuang, L. Wang, Y. Zhang, J. Li, G. Wang, Controlled synthesis of cobalt nanparticles on the carbon spheres and Fischer-Tropsch synthesis performance, J. Mol. Sci. 35 (01) (2019) 76–82.
[27] Y. Wang, Z. Yang, L. Gao, Theoretical study of electronic properties of phenyl covalent functional carbon nanotubes, J. Mol. Sci. 32 (2016) 259–264.
[28] Z. Yang, X. Liu, W. Xiang, M. Luo, Y. Yang, Y. Guo, Preparation of g-C3N4/TiO2 film-coated optical fiber bundles and degradation property of meta-xylene, J. Mol. Sci. 34 (03) (2018) 199–206.
[29] M. Zhou, S. Guo, Electrocatalytic interface based on novel carbon nanomaterials for advanced electrochemical sensors, ChemCatChem 7 (18) (2015) 2744–2764.
[30] J. Wang, Carbon-nanotube based electrochemical biosensors: a review, Electroanalysis 17 (1) (2005) 7–14.
[31] L. Ding, B. Zou, Y. Li, H. Liu, Z. Wang, C. Zhao, Y. Su, Y. Guo, The production of hydrochar-based hierarchical porous carbons for use as electrochemical supercapacitor electrode materials, Colloids Surf. A: Physicochem. Eng. Asp. 423 (2013) 104–111.
[32] L. Zhu, C. Tian, R. Yang, J. Zhai, Anodic stripping voltammetric determination of lead in tap water at an ordered mesoporous carbon/Nafion composite film electrode, Electroanalysis 20 (5) (2008) 527–533.
[33] Q. Wu, D. Gong, Z. Luan, K. Li, P. Ye, T. Tang, Research on preparation and properties of the adsorption materials based on molecular sieves against the NH3, J. Mol. Sci. 34 (01) (2018) 21–25.
[34] X. Song, Y. Lan, Y. Wei, W. Yuan, C. Dong, Preparation of Ti/Ag + Cu electrode and application on degradation of salicylic acid, J. Mol. Sci. 34 (05) (2018) 353–358 (+5).
[35] J. Gao, Y. Jia, N. Gu, K. Zhao, K. Wang, B. Zhang, Preparation of ZIF-8 and its application as carrier for bactericidal drug, J. Mol. Sci. 34 (04) (2018) 324–330.
[36] P. He, X. Li, L. Wang, H. Wang, Bis-pyrene based self-assembled nanomaterials: in situ construction, transformation and biomedical effects, J. Mol. Sci. 34 (02) (2018) 89–102.
[37] L. Yu, Y. Wang, R. Xu, Z. Chen, D. Zhou, Fabrication of SiW_(12)/g-C_3N_4 nanocomposites and their photocatalytic activity, J. Mol. Sci. 34 (03) (2018) 177–182.
[38] H. Kroto, J. Heath, S. O'brien, R. Curl, R. Smalley, This week's citation classic®, Nature 318 (1985) 162–163.
[39] C.N.R. Rao, A.K. Sood, K.S. Subrahmanyam, A. Govindaraj, Graphene: the new two-dimensional nanomaterial, Angew. Chem. Int. Ed. 48 (42) (2009) 7752–7777.
[40] K.M. Zeinu, H. Hou, B. Liu, X. Yuan, L. Huang, X. Zhu, J. Hu, J. Yang, S. Liang, X. Wu, A novel hollow sphere bismuth oxide doped mesoporous carbon nanocomposite material derived from sustainable biomass for picomolar electrochemical detection of lead and cadmium, J. Mater. Chem. A 4 (36) (2016) 13967–13979.
[41] L. Zhang, Z. Liu, G. Cui, L. Chen, Biomass-derived materials for electrochemical energy storages, Prog. Polym. Sci. 43 (1) (2015) 136–164.
[42] S. Deng, B. Hu, T. Chen, B. Wang, J. Huang, Y. Wang, G. Yu, Activated carbons prepared from peanut shell and sunflower seed shell for high CO2 adsorption, Adsorption 21 (1–2) (2015) 125–133.
[43] F. Pan, Z. Cao, Q. Zhao, H. Liang, J. Zhang, Nitrogen-doped porous carbon nanosheets made from biomass as highly active electrocatalyst for oxygen reduction reaction, J. Power Sources 272 (2014) 8–15.
[44] L. Wang, Q. Zhang, S. Chen, F. Xu, S. Chen, J. Jia, H. Tan, H. Hou, Y. Song, Electrochemical sensing and biosensing platform based on biomass-derived macroporous carbon materials, Anal. Chem. 86 (3) (2014) 1414–1421.
[45] K. Xiao, L.-X. Ding, H. Chen, S. Wang, X. Lu, H. Wang, Nitrogen-doped porous carbon derived from residuary shaddock peel: a promising and sustainable anode for high energy density asymmetric supercapacitors, J. Mater. Chem. A 4 (2) (2016) 372–378.
[46] S. De, A.M. Balu, J.C. van der Waal, R. Luque, Biomass-derived porous carbon materials: synthesis and catalytic applications, ChemCatChem 7 (11) (2015) 1608–1629.
[47] A. Jain, R. Balasubramanian, M. Srinivasan, Production of high surface area mesoporous activated carbons from waste biomass using hydrogen peroxide-mediated hydrothermal treatment for adsorption applications, Chem. Eng. J. 273 (2015) 622–629.
[48] R. Madhu, K.V. Sankar, S.-M. Chen, R.K. Selvan, Eco-friendly synthesis of activated carbon from dead mango leaves for the ultrahigh sensitive detection of toxic heavy metal ions and energy storage applications, RSC Adv. 4 (3) (2014) 1225–1233.
[49] T. Yang, T. Qian, M. Wang, X. Shen, N. Xu, Z. Sun, C. Yan, A sustainable route from biomass byproduct okara to high content nitrogen-doped carbon sheets for efficient sodium ion batteries, Adv. Mater. 28 (3) (2016) 539–545.
[50] X. Li, Y. Wang, J. Liu, M. Sun, X. Bo, H.-L. Wang, M. Zhou, Amperometric ascorbic acid biosensor based on carbon nanoplatelets derived from ground cherry husks, Electrochem. Commun. 82 (2017) 139–144.
[51] R. Liu, L. Wan, S. Liu, L. Pan, D. Wu, D. Zhao, An interface-induced co-assembly approach towards ordered mesoporous carbon/graphene aerogel for high--performance supercapacitors, Adv. Funct. Mater. 25 (4) (2015) 526–533.
[52] J. Wei, D. Zhou, Z. Sun, Y. Deng, Y. Xia, D. Zhao, A controllable synthesis of rich nitrogen-doped ordered mesoporous carbon for CO_2 capture and supercapacitors, Adv. Funct. Mater. 23 (18) (2013) 2322–2328.
[53] L. Sun, C. Tian, M. Li, X. Meng, L. Wang, R. Wang, J. Yin, H. Fu, From coconut shell to porous graphene-like nanosheets for high-power supercapacitors, J. Mater. Chem. A 1 (21) (2013) 6462–6470.
[54] D.C. Marcano, D.V. Kosynkin, J.M. Berlin, A. Sinitskii, Z. Sun, A. Slesarev, L.B. Alemany, W. Lu, J.M. Tour, Improved synthesis of graphene oxide, ACS Nano 4 (8) (2010) 4806–4814.
[55] G. Wang, H. Wang, X. Lu, Y. Ling, M. Yu, T. Zhai, Y. Tong, Y. Li, Solid-state supercapacitor based on activated carbon cloths exhibits excellent rate capability, Adv. Mater. 26 (17) (2014) 2676–2682.
[56] K. Wang, H. Wang, S. Ji, H. Feng, V. Linkov, R. Wang, Biomass-derived activated carbon as high-performance non-precious electrocatalyst for oxygen reduction, RSC Adv. 3 (30) (2013) 12039–12042.
[57] R. Wang, T. Zhou, H. Li, H. Wang, H. Feng, J. Goh, S. Ji, Nitrogen-rich mesoporous carbon derived from melamine with high electrocatalytic performance for oxygen reduction reaction, J. Power Sources 261 (2014) 238–244.
[58] J. Dong, D.A. Drabold, Ring formation and the structural and electronic properties of tetrahedral amorphous carbon surfaces, Phys. Rev. B 57 (24) (1998) 15591.
[59] T. Bordjiba, M. Mohamedi, L.H. Dao, New Class of Carbon-Nanotube Aerogel Electrodes for Electrochemical Power Sources, Adv. Mater. 20 (4) (2008) 815–819.
[60] J.-z. Zou, X.-r. Zeng, X.-b. Xiong, H.-l. Tang, L. Li, Q. Liu, Z.-q. Li, Preparation of vapor grown carbon fibers by microwave pyrolysis chemical vapor deposition, Carbon 45 (4) (2007) 828–832.
[61] N. Jia, Z. Wang, G. Yang, H. Shen, L. Zhu, Electrochemical properties of ordered mesoporous carbon and its electroanalytical application for selective determination of dopamine, Electrochem. Commun. 9 (2) (2007) 233–238.
[62] R. Wang, X. Li, H. Li, Q. Wang, H. Wang, W. Wang, J. Kang, Y. Chang, Z. Lei, Highly stable and effective Pt/carbon nitride (CNx) modified SiO2 electrocatalyst for oxygen reduction reaction, Int. J. Hydrog. Energy 36 (10) (2011) 5775–5781.
[63] J. Bai, X. Bo, D. Zhu, G. Wang, L. Guo, A comparison of the electrocatalytic activities of ordered mesoporous carbons treated with either HNO3 or NaOH, Electrochim. Acta 56 (2) (2010) 657–662.
[64] N. Sankararamakrishnan, D. Chauhan, J. Dwivedi, Synthesis of functionalized carbon nanotubes by floating catalytic chemical vapor deposition method and their sorption behavior toward arsenic, Chem. Eng. J. 284 (2016) 599–608.
[65] R.S. Nicholson, Theory and application of cyclic voltammetry for measurement of electrode reaction kinetics, Anal. Chem. 37 (11) (1965) 1351–1355.
[66] J. De Lange, Harold H. Kelley, John W. Thibaut (Eds.), Interpersonal Relations: A Theory of Interdependence, John Wiley & Sons, New York, 1978, p. 341 (pp. $18.95, Oxford University Press, 1980).
[67] S.S. Kumar, S.S. Narayanan, Amperometric sensor for the determination of ascorbic acid based on cobalt hexacyanoferrate modified electrode fabricated through a new route, Chem. Pharm. Bull. 54 (7) (2006) 963–967.
[68] A. Sivanesan, P. Kannan, S.A. John, Electrocatalytic oxidation of ascorbic acid using a single layer of gold nanoparticles immobilized on 1, 6-hexanedithiol modified gold electrode, Electrochim. Acta 52 (28) (2007) 8118–8124.
[69] A. Mohadesi, M.A. Taher, Electrochemical behavior of Naphthol green B doped in polypyrrole film and its application for electrocatalytic oxidation of ascorbic acid, Sens. Actuators B: Chem. 123 (2) (2007) 733–739.
[70] F. Li, C. Tang, S. Liu, G. Ma, Development of an electrochemical ascorbic acid sensor based on the incorporation of a ferricyanide mediator with a polyelectrolyte–calcium carbonate microsphere, Electrochim. Acta 55 (3) (2010) 838–843.
[71] B. Habibi, M.H. Pournaghi-Azar, Simultaneous determination of ascorbic acid, dopamine and uric acid by use of a MWCNT modified carbon-ceramic electrode and differential pulse voltammetry, Electrochim. Acta 55 (19) (2010) 5492–5498.
[72] S. Zhang, Y. Fu, C. Sun, Fabrication of poly (allylamine) ferrocene monolayer based on electrostatic interaction and its electrocatalytic oxidation of ascorbic acid, Electroanalysis 15 (8) (2003) 739–746.
[73] L. Xi, D. Ren, J. Luo, Y. Zhu, Electrochemical analysis of ascorbic acid using copper nanoparticles/polyaniline modified glassy carbon electrode, J. Electroanal. Chem. 650 (1) (2010) 127–134.
[74] J.C.K. Mbouguen, I.T. Kenfack, A. Walcarius, E. Ngameni, Electrochemical response of ascorbic and uric acids at organoclay film modified glassy carbon electrodes and sensing applications, Talanta 85 (1) (2011) 754–762.
[75] A.B. Florou, M.I. Prodromidis, S.M. Tzouwara-Karayanni, M.I. Karayannis, Fabrication and voltammetric study of lanthanum 2, 6-dichlorophenolindophenol chemically modified screen printed electrodes: application for the determination of ascorbic acid, Anal. Chim. Acta 423 (1) (2000) 107–114.
[76] X. Sui, X. Feng, J. Song, M.A. Hempenius, G.J. Vancso, Electrochemical sensing by surface-immobilized poly (ferrocenylsilane) grafts, J. Mater. Chem. 22 (22) (2012) 11261–11267.
[77] D. Wen, S. Guo, S. Dong, E. Wang, Ultrathin Pd nanowire as a highly active electrode material for sensitive and selective detection of ascorbic acid, Biosens. Bioelectron. 26 (3) (2010) 1056–1061.
[78] M. Zhou, L.-P. Guo, Y. Hou, X.-J. Peng, Immobilization of Nafion-ordered mesoporous carbon on a glassy carbon electrode: application to the detection of epinephrine, Electrochim. Acta 53 (12) (2008) 4176–4184.